

A Digital Twin of the Angiotensin II Receptor Blocker Losartan: Physiologically Based Modeling of Blood Pressure Regulation

Ennie TENSIL ¹  and Matthias KÖNIG ^{2,*} 

¹ Charité – Universitätsmedizin Berlin, corporate member of Freie Universität Berlin and Humboldt-Universität zu Berlin, Charitéplatz 1, 10117 Berlin, Germany

² Humboldt-Universität zu Berlin, Faculty of Life Sciences, Department of Biology, Institute of Theoretical Biology, Systems Medicine of the Liver, Unter den Linden 6, 10099 Berlin, Germany

* Correspondence: koenigmx@hu-berlin.de

Abstract: Losartan, a commonly prescribed angiotensin II receptor blocker (ARB) used to treat hypertension and heart failure, shows significant variability in pharmacokinetics (PK) and pharmacodynamics (PD) among individuals. In this study, we developed a physiologically based pharmacokinetic/pharmacodynamic (PBPK/PD) model of losartan and its active metabolite, E3174, using curated data from 24 clinical trials. The model, implemented in SBML, mechanistically describes the processes of absorption, hepatic metabolism, renal excretion, and pharmacodynamic regulation via the renin–angiotensin–aldosterone system (RAAS). Simulation studies examined the effects of dose, hepatic and renal impairment, and genetic polymorphisms in CYP2C9 and ABCB1 on the model. The model successfully reproduced key PK/PD observations, including dose-dependent receptor blockade, attenuated responses with hepatic impairment, modest enhancement with renal impairment, and substantial variability in E3174 formation dependent on CYP2C9; the effects of ABCB1 were minimal. This mechanistic digital twin framework provides a quantitative basis for understanding variability in losartan therapy and supports its application in individualized dosing strategies.

Keywords: Losartan; Angiotensin II Receptor Blocker; ARB; PBPK/PD modeling; Pharmacokinetics; Pharmacodynamics; SBML

1. Introduction

Hypertension, defined as blood pressure of 130 mmHg or higher and/or a diastolic blood pressure of 80 mmHg or higher, is a major global health challenge and leading risk factor for cardiovascular disease, stroke, and kidney failure [1–3]. In 2019, over 1.2 billion people worldwide were affected, with prevalence exceeding 50% in some regions [2]. Despite its silent clinical course, hypertension contributes to over 8 million deaths annually [3]. Risk factors include age, genetics, obesity, inactivity, and unhealthy diet [1]. While treatment options exist, improved prevention and personalized therapies remain essential.

The renin-angiotensin-aldosterone system (RAAS) regulates blood pressure and fluid balance. Renin release from the kidney cleaves angiotensinogen to angiotensin I, which is converted by the angiotensin converting enzyme (ACE) into angiotensin II [4]. Angiotensin II raises blood pressure via vasoconstriction, stimulation of aldosterone and vasopressin release, enhanced sodium reabsorption, and increased sympathetic tone [5]. Dysregulation of the RAAS underlies hypertension, heart failure, and kidney disease.

Pharmacological treatments target RAAS at multiple points. Beta-blockers lower renin, direct renin inhibitors (e.g., aliskiren) block its activity, ACE inhibitors (e.g., ramipril) prevent angiotensin II formation, and angiotensin II receptor blockers (ARBs) (e.g., losartan) selectively antagonize AT1 receptors [5–8]. ARBs offer high specificity by blocking receptor-mediated effects of angiotensin II

without interfering with its synthesis. Other antihypertensive drug classes include diuretics and calcium channel blockers [9,10].

Losartan, the first ARB approved in 1995, is widely prescribed for hypertension and related complications [11,12]. By competitively blocking AT1 receptors, it reduces vasoconstriction, aldosterone secretion, and water retention. Its major active metabolite, E3174, is generated through CYP2C9 mediated conversion and 10–40 times more potent [13], though losartan itself remains an effective antagonist. Both compounds contribute to clinical efficacy. Losartan is well tolerated, with dizziness and mild respiratory symptoms as the most common side effects [12]. It is available as monotherapy or combined with hydrochlorothiazide for greater blood pressure reduction [14]. Standard dosing ranges from 25–100 mg/day. Like other ARBs, it is contraindicated in pregnancy [11].

Losartan shows rapid oral absorption, with peak plasma levels after 1–2 h and bioavailability of about 33% due to first-pass metabolism [13,15]. E3174 peaks later (3–4 h) and has 4–8-fold higher systemic exposure [13,16]. Both compounds bind strongly to plasma proteins and are eliminated via hepatic metabolism and renal/fecal excretion, with terminal half-lives of ~2 h (losartan) and 4–6 h (E3174) [17,18]. Only small fractions are excreted unchanged renally [19]. Minor metabolites such as L158 reflect additional metabolic pathways [18,20].

Pharmacodynamically, losartan lowers blood pressure by blocking AT1 receptors, thereby reducing aldosterone secretion [21–23]. AT1 blockade also increases renin and angiotensin levels due to loss of feedback control [24,25]. Enhanced stimulation of AT2 receptors may further contribute to vasodilation [26].

Liver cirrhosis reduces losartan clearance by about 50% and doubles bioavailability, leading to higher plasma levels, though E3174 exposure increases only modestly [11,27]. Renal impairment decreases clearance of losartan and E3174 but generally does not elevate E3174 levels due to compensatory mechanisms [19,28,29]. Neither compound is dialyzable, and dose adjustments are mainly required in hepatic dysfunction [30].

Drug response varies due to genetic polymorphisms in ABCB1 and CYP2C9 genes. Variants of ABCB1, a gene encoding for a drug efflux transporter also known as P-glycoprotein or MDR1, influence losartan absorption and blood pressure response, though findings are inconsistent [31–33]. CYP2C9 polymorphisms (*2, *3, *13) reduce metabolism to E3174, increasing losartan exposure and diminishing therapeutic effect [13,34–37]. The frequency of these alleles varies by population [38–40].

Physiologically-based pharmacokinetic/ pharmacodynamic (PBPK/PD) models integrate ADME processes (absorption, distribution, metabolism and elimination) with drug effects using differential equations [41]. They allow simulation of dosing regimens, organ dysfunction, and genetic variability on drug behavior. In this work, a PBPK/PD model of losartan was developed to investigate dose-dependent PK/PD effects, the influence of hepatic and renal impairment and the impact of ABCB1 and CYP2C9 variants. The aim is to clarify sources of variability in losartan response and support individualized therapy.

2. Materials and Methods

2.1. Systematic literature research

A systematic literature search was performed in PubMed and PKPDAI [42] on 27 August 2024 using the terms losartan AND pharmacokinetics. Eligible studies included human clinical trials with PK/PD data in healthy volunteers, hepatic/renal impairment, or CYP2C9 genotypes. Excluded were animal studies, pediatric/ single-patient reports, reviews, computational models, cocktail or combination designs, and PD-only studies. Where data were redundant, representative studies were selected. Additional *in vitro* reports were included to derive kinetic parameters.

2.2. Data curation

Relevant study data were curated into PK-DB [43]. Extracted metadata included group and individual characteristics (age, sex, genotype, comorbidities), interventions (dose, route, regimen), and

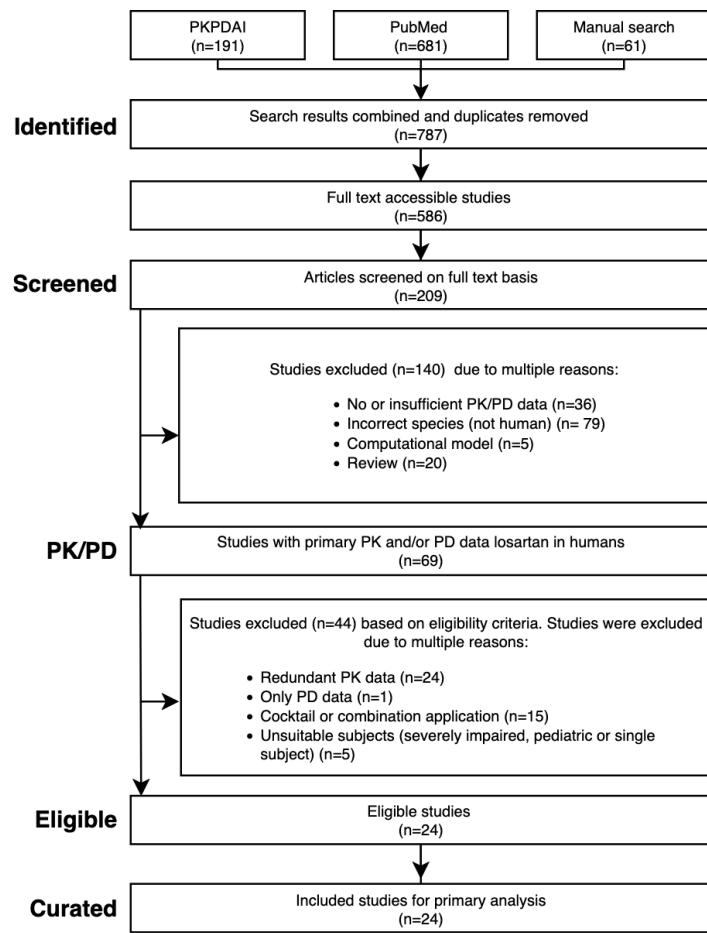


Figure 1. PRISMA flow diagram of the literature search and study selection process.

outcomes (concentration-time profiles of losartan and metabolites, RAAS biomarkers, blood pressure, heart rate). Digitization of graphical data was performed using WebPlotDigitizer [44]. Data were organized according to PK-DB standards into groups, individuals, interventions, and time courses, providing the heterogeneous dataset used for modeling and validation.

2.3. Computational model

A physiologically-based pharmacokinetic/pharmacodynamic (PBPK/PD) model was built in the Systems Biology Markup Language (SBML) [45,46] using sbmlutils [47], visualized using cysbml [48], simulated with sbmlsim [49] based on libroadrunner [50,51], and shared under CC-BY 4.0 at Zenodo (v0.7.1) [52]. The model consists of submodels for intestine, liver, kidney, and RAAS, connected by systemic circulation. Hepatic impairment was implemented as progressive cirrhosis [53,54], aligned with Child-Pugh classes [55,56]. Renal impairment was modeled as reduced clearance based on glomerular filtration rate following KDIGO guidelines [57,58]. CYP2C9 genetic variability was incorporated using allele-specific activity scaling [59–61], and ABCB1 activity was adjusted according to published polymorphism data [62,63].

2.4. Parameter optimization

Model parameters were estimated by minimizing weighted residuals between clinical data and simulations. The cost function was defined as

$$F(\vec{p}) = 0.5 \sum_{i,k} (w_{i,k} \cdot r_{i,k}(\vec{p}))^2,$$

with weights $w_{i,k} = n_k / \sigma_{i,k}$ based on study size and measurement error. One hundred optimization runs with varying initial conditions were performed. Fitting proceeded in two stages: first pharmacokinetic, then pharmacodynamic parameters. Independent datasets including multiple dosing and impairment scenarios were used for validation.

2.5. Pharmacokinetic and pharmacodynamic parameters

Pharmacokinetic parameters for losartan, E3174, and L158 were derived using non-compartmental methods. The elimination rate (k_{el}) was estimated from log-linear regression of the terminal phase. The area under the concentration-time curve (AUC) was computed by trapezoidal rule and extrapolation. Apparent clearance (Cl/F) and volume of distribution (V_d/F) were derived from $Cl/F = k_{el} \cdot V_d$ and $V_d/F = D/(AUC_\infty \cdot k_{el})$, where D is dose. Pharmacodynamic outputs (renin, angiotensin, aldosterone, blood pressure) were summarized by maximal and minimal values.

3. Results

3.1. Losartan Database

An open database containing pharmacokinetic and pharmacodynamic data of losartan from 24 clinical studies was compiled, covering a range of dosing regimens, physiological conditions and different genotypes (Table 1). This dataset served as the basis for developing the losartan PBPK/PD model.

Table 1. Summary of studies for modeling. Overview of study identifiers, PK-DB IDs, administered substance and administration route, dosing regimens, doses [mg], and subject characteristics, including health status, renal functional impairment (RFI), hepatic functional impairment (HFI), and the studied genotypes (CYP2C9, ABCB1).

Study	PK-DB	Substance	Route	Dosing	Dose [mg]	Healthy RFI	HFI	CYP2C9 ABCB1
Bae2011 [64]	PKDB00895	losartan potassium	po	single	50	✓		✓
Donzelli2014 [65]	PKDB00953	losartan	po	single	12.5	✓		✓
FDA1995S60 [18]	PKDB00965	C14 losartan, e3174	po/iv, iv	single	100/30, 20	✓		
FDA1995S67 [18]	PKDB00966	losartan, e3174	po/iv, iv	single	50/10, 10		✓	
Fischer2002 [37]	PKDB00894	losartan	po	multi	50	✓		✓
Han2009a [66]	PKDB00909	losartan potassium	po	single	50	✓		✓
Huang2021 [67]	PKDB00919	losartan potassium	po	single	50	✓		✓
Kim2016 [68]	PKDB00896	losartan	po	single	50	✓		
Kobayashi2008 [69]	PKDB00920	losartan potassium	po	single	25	✓		
Lee2003b [70]	PKDB00899	losartan potassium	po	single	50	✓		✓
Liz2009 [40]	PKDB00912	losartan	po	single	50	✓		✓
Lo1995 [13]	PKDB00922	losartan potassium, e3174	po/iv	single	50, 100/20, 30	✓		
Munafio1992 [71]	PKDB00921	losartan	po	single	40, 80, 120	✓		
Oh2012 [72]	PKDB00054	losartan	po	single	2	✓		
Ohtawa1993 [16]	PKDB00911	losartan	po	single, multi	25, 50, 100, 200	✓		
Paris2019 [73]	PKDB00642	losartan potassium	po	single	12.5			
Sekino2003 [36]	PKDB00961	losartan	po	single	25	✓		✓
Shin2020 [32]	PKDB00898	losartan potassium	po	single	50	✓		
Sica1995 [19]	PKDB00910	losartan	po	multi	100		✓	
Tanaka2014 [74]	PKDB00136	losartan	po	single	50	✓		
Yasar2002a [35]	PKDB00897	losartan	po	single	50	✓		✓

3.2. Computational Model

A PBPK/PD model of losartan was created that includes key factors that determine intra- and inter-individual variability (Figure 2). The model includes the organs involved in the pharmacokinetics of losartan (gastrointestinal tract, liver, and kidney), connected through the systemic circulation, as well as the main pharmacodynamic outputs of the RAAS (renin, angiotensin I, aldosterone, systolic and diastolic blood pressure). The main patient-specific factors that are known to affect the pharmacokinetics and pharmacodynamics of losartan are included in the model. Specifically, four key factors were included: dose dependency, liver impairment, renal impairment, and genotype variability.

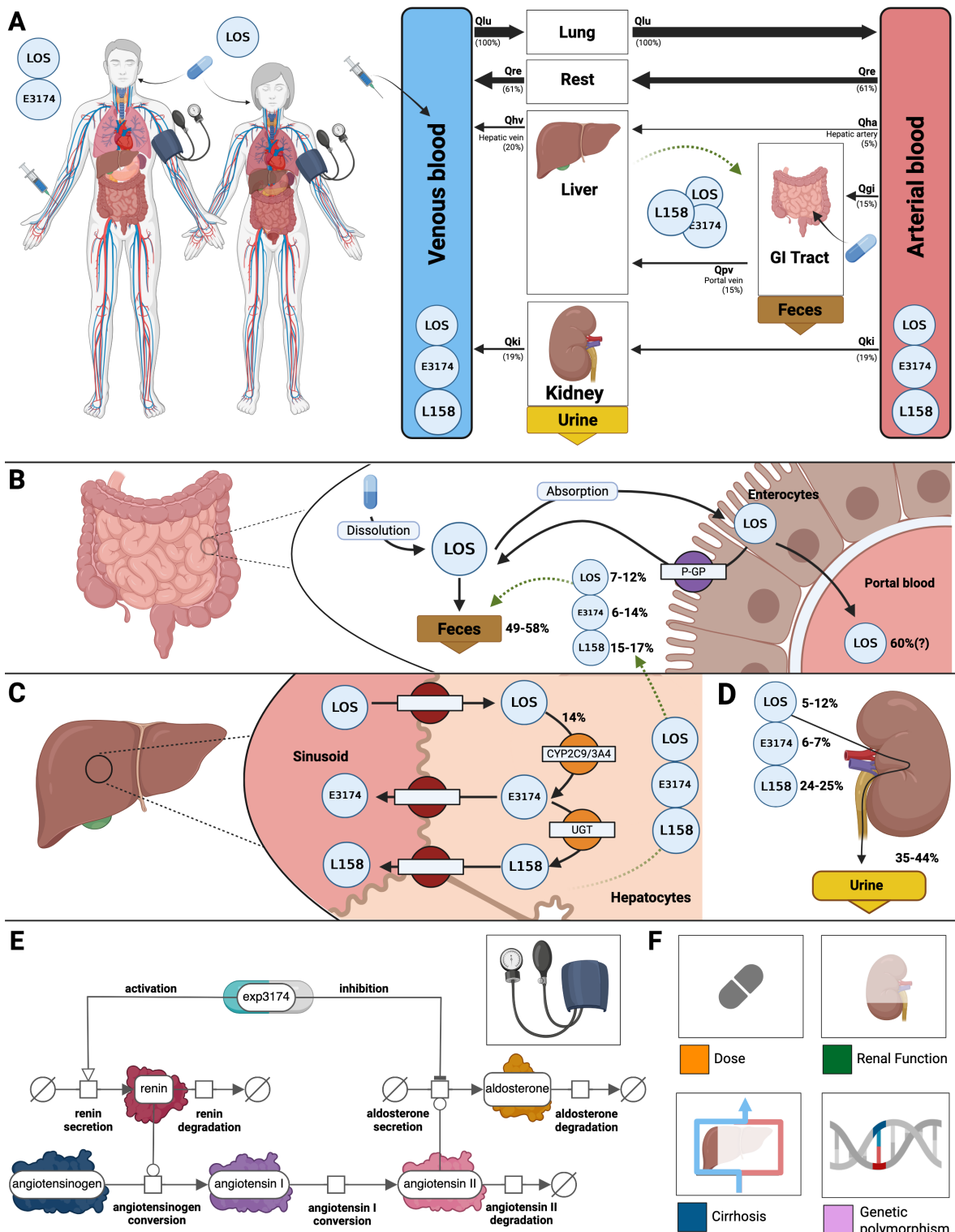


Figure 2. Overview of the physiologically-based model of losartan. (A) Whole body model showing circulation via the arterial and venous blood, with organs (liver, GI tract, kidney) influencing the pharmacokinetics of losartan (LOS). (B) Intestine model illustrating the dissolution and absorption of LOS by enterocytes and the P-glycoprotein mediated efflux back into the intestine. Approximately 49-58% of the dose is excreted as losartan or metabolites (E3174 and L158). (C) Hepatic model depicting the uptake of losartan by hepatocytes and its conversion by cytochrome p450 2C9 and 3A4 (CYP2C9, CYP3A4) to losartan carboxylic acid E3174 (14% of losartan dose) and the following conversion by UDP-glucuronosyltransferase (UGT) to L158. Losartan and its metabolites can also re-enter the intestinal model via enterohepatic circulation (biliary export). (D) Renal model showing excretion of losartan, E3174 and L158 via urine, approximately 5-12%, 6-7% and 24-25%, respectively. (E) Pharmacodynamic model of E3174 acting on the RAAS. (F) Key factors influencing losartan PK and PD profiles accounted for in the model. Illustrations for losartan dosing, hepatic impairment, renal impairment and genetic polymorphisms.

3.3. Dose Dependency

Dose-dependent behavior of the losartan PBPK/PD model was assessed by simulating oral doses between 10 and 100 mg (Figure 3). The model captures the pharmacokinetics of losartan and its active metabolite E3174 in plasma, urine, and feces, as well as the associated pharmacodynamic responses (aldosterone, renin, angiotensin I, and blood pressure). Simulations reproduced key dose-related trends: increasing exposure with dose, a decreasing E3174/losartan ratio at higher doses, nonlinear increases in AUC and C_{max} (particularly for E3174), and dose-dependent prolongation of E3174 half-life. On the pharmacodynamic level, higher doses produced stronger suppression of aldosterone and blood pressure, accompanied by compensatory increases in renin and angiotensin I. These patterns are consistent with findings from published clinical studies (Figure 3 and 4).

3.4. Hepatic Impairment

Figure 5 shows the impact of hepatic dysfunction on the pharmacokinetics and pharmacodynamics of losartan and E3174. As cirrhosis severity increases, losartan plasma and urine concentrations rise, while E3174 levels and the E3174/losartan ratio decrease. Fecal excretion remains largely unchanged, indicating that hepatic impairment predominantly affects metabolic clearance rather than biliary elimination.

Pharmacokinetic analysis reveals increasing AUC, C_{max} , and half-life for both losartan and E3174 with worsening cirrhosis, accompanied by a decline in the elimination rate constant (kel). While losartan accumulation is qualitatively consistent with clinical observations from patients with mild to moderate cirrhosis [8,11], the model underestimates absolute concentrations, particularly for E3174, which shows a delayed but modest increase in plasma levels at higher cirrhosis degrees. This discrepancy likely reflects unaccounted factors such as reduced hepatic blood flow, altered enzyme activity, or additional compensatory mechanisms [27].

Pharmacodynamically, impaired liver function attenuates the formation of E3174 and modifies RAAS regulation. Early renin and angiotensin I responses are reduced, while aldosterone and blood pressure increase initially, with prolonged elevation in more severe cirrhosis. These trends correspond to delayed normalization of hormonal and hemodynamic parameters. Despite sparse PD data and limited control groups, the model reproduces general concentration–time and dose–response patterns, supporting the clinical recommendation of dose adjustment in hepatic impairment. This is particularly relevant for patients with comorbidities such as heart failure, where sensitivity to RAAS inhibition is increased [35,36].

3.5. Renal Impairment

Figure 6 illustrates the effect of declining renal function on the pharmacokinetics and pharmacodynamics of losartan and its active metabolite E3174. As renal function decreases, losartan plasma concentrations remain largely unchanged, whereas E3174 levels increase, accompanied by reduced urinary excretion of both compounds. Fecal excretion of losartan shows a slight compensatory rise, and the E3174/losartan ratio increases with impaired renal clearance.

On the pharmacokinetic level, the model predicts stable AUC and C_{max} values for losartan, while E3174 shows rising AUC, C_{max} , and half-life as renal function declines, reflecting reduced clearance. These results align qualitatively with the physiology of renal elimination, though they overestimate metabolite accumulation compared to clinical findings [19,28], where E3174 exposure remained stable across renal function groups. This discrepancy may indicate unaccounted processes such as altered absorption, metabolism, or hepatic clearance of E3174 [11].

Pharmacodynamically, impaired renal function amplifies losartan's antihypertensive effects. The model predicts stronger suppression of aldosterone and systolic blood pressure, along with compensatory rises in renin and angiotensin I. While direct PD data in renally impaired populations are limited, these predictions are physiologically plausible and extend clinical observations. Nevertheless,

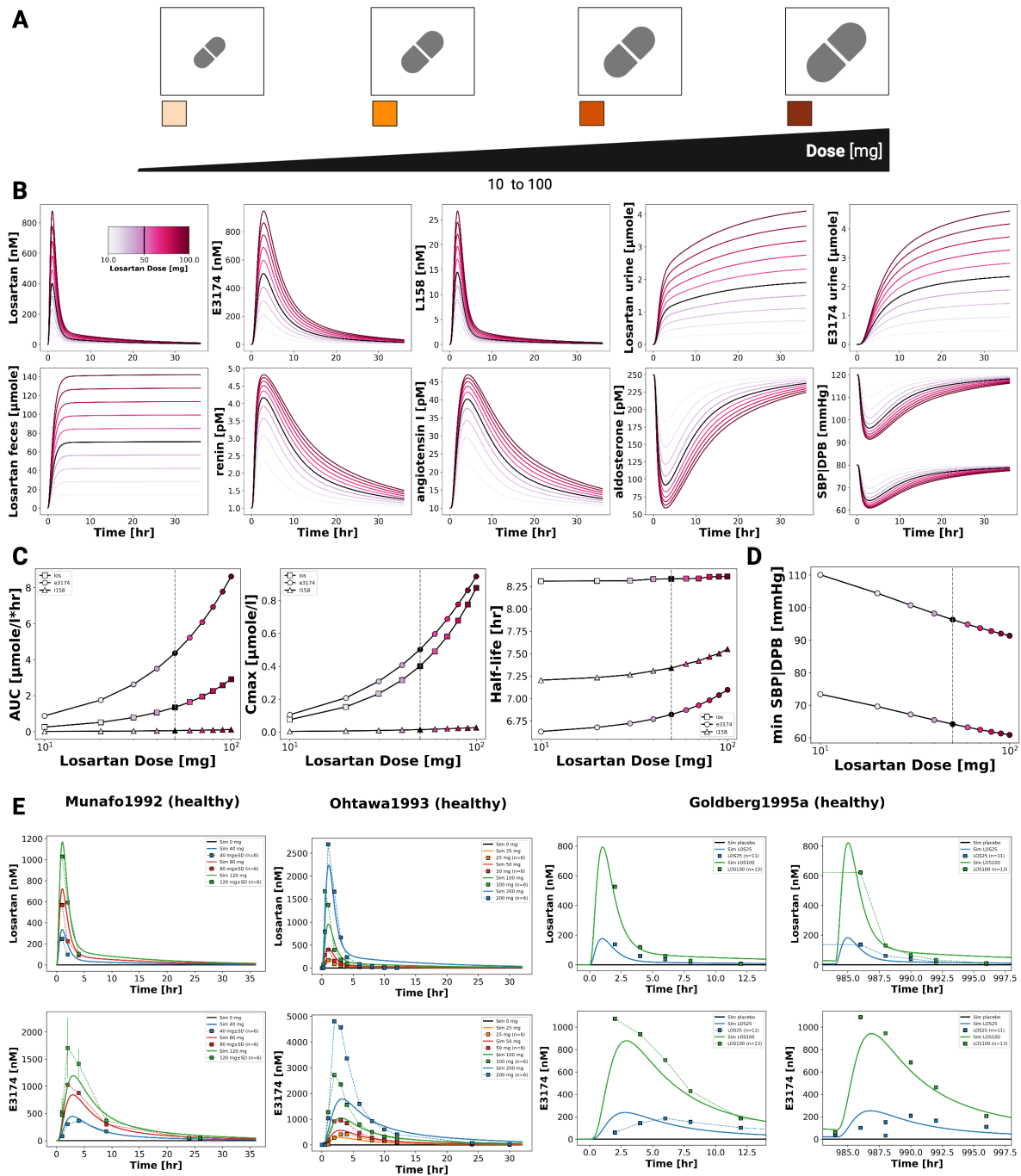


Figure 3. Dose-dependent pharmacokinetics and pharmacodynamics of losartan. (A) Illustration of the losartan dose range (10–100 mg) evaluated in the simulations. (B) Simulated plasma concentrations profiles of losartan, E3174 and L158, urinary excretion profile of losartan and E3174, a fecal excretion profile of losartan as well as simulated RAAS biomarkers (renin, angiotensin I and aldosterone) and blood pressure responses across doses (10–100 mg). Dose intensity is indicated by line color. (C) Dose–response curves for AUC, C_{max} and half-life. (D) Dose dependent maximum or minimum values of systolic blood pressure SBP and diastolic blood pressure DBP. (E) Simulated versus observed losartan pharmacokinetics. Data from [16,71,75].

the degree of RAAS suppression may be slightly overestimated due to the absence of compensatory mechanisms such as altered hepatic clearance or long-term feedback regulation [36,37,77].

3.6. ABCB1 Genotypes

Figure 7 illustrates the influence of ABCB1 (P-glycoprotein) transporter activity on the pharmacokinetics and pharmacodynamics of losartan and E3174. Simulations across varying transporter

171

172

173

174

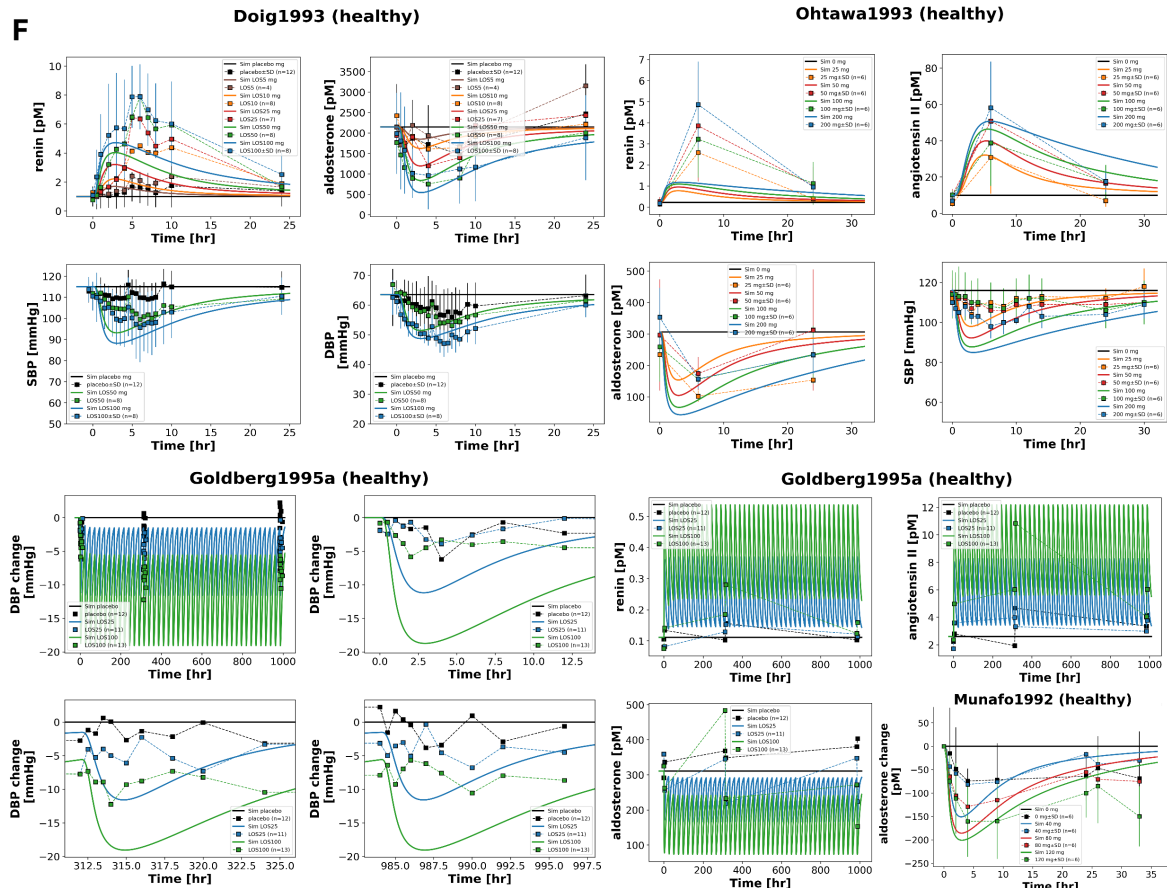


Figure 4. continued: Dose-dependent pharmacokinetics and pharmacodynamics of losartan. (F) Simulated versus observed losartan pharmacodynamics. Data from [16,71,75,76].

activity levels, including common diplotypes (GG/CC, GT/CT, TT/TT), show that reduced ABCB1 activity leads to increased plasma and urinary concentrations of both compounds, while fecal excretion of losartan declines due to decreased intestinal and biliary efflux. 176

Pharmacokinetic analysis indicates modest increases in AUC and C_{max} for losartan and E3174 with lower ABCB1 activity, whereas elimination rate constants (kel) and half-life remain largely unchanged. 177
The plasma and urine E3174/losartan ratio decreases slightly under low transporter activity. These 178
trends are qualitatively consistent with clinical observations [32], although absolute concentrations 179
are slightly underestimated by the model. 180

Pharmacodynamically, reduced ABCB1 activity slightly enhances RAAS-related effects, including 181
modest increases in renin and angiotensin I and marginal reductions in aldosterone and blood pressure. 182
While these changes are small and unlikely to necessitate dose adjustments based on ABCB1 diplotype 183
alone, the model demonstrates the capacity to predict subtle genotype-dependent differences in drug 184
exposure and pharmacodynamic response. Future refinement could include better representation of 185
renal P-gp expression and its contribution to systemic clearance, as well as additional clinical data on 186
pharmacodynamic outcomes to improve predictive accuracy [32]. 187

3.7. CYP2C9 Genotypes

Figure 8 illustrates the impact of CYP2C9 genetic variability on the pharmacokinetics and pharmacodynamics of losartan and its active metabolite E3174. Simulations across a continuous range of CYP2C9 activity, as well as genotype-specific simulations for *1/*1, *1/*2, *1/*3, *1/*13, *2/*2, *2/*3, and *3/*3, demonstrate that reduced enzyme activity leads to impaired metabolic conversion, resulting in higher plasma, urine, and fecal levels of losartan and decreased E3174 exposure. 191

176
177
178
179
180
181
182
183
184
185
186
187
188
189
190
191
192
193
194
195
196

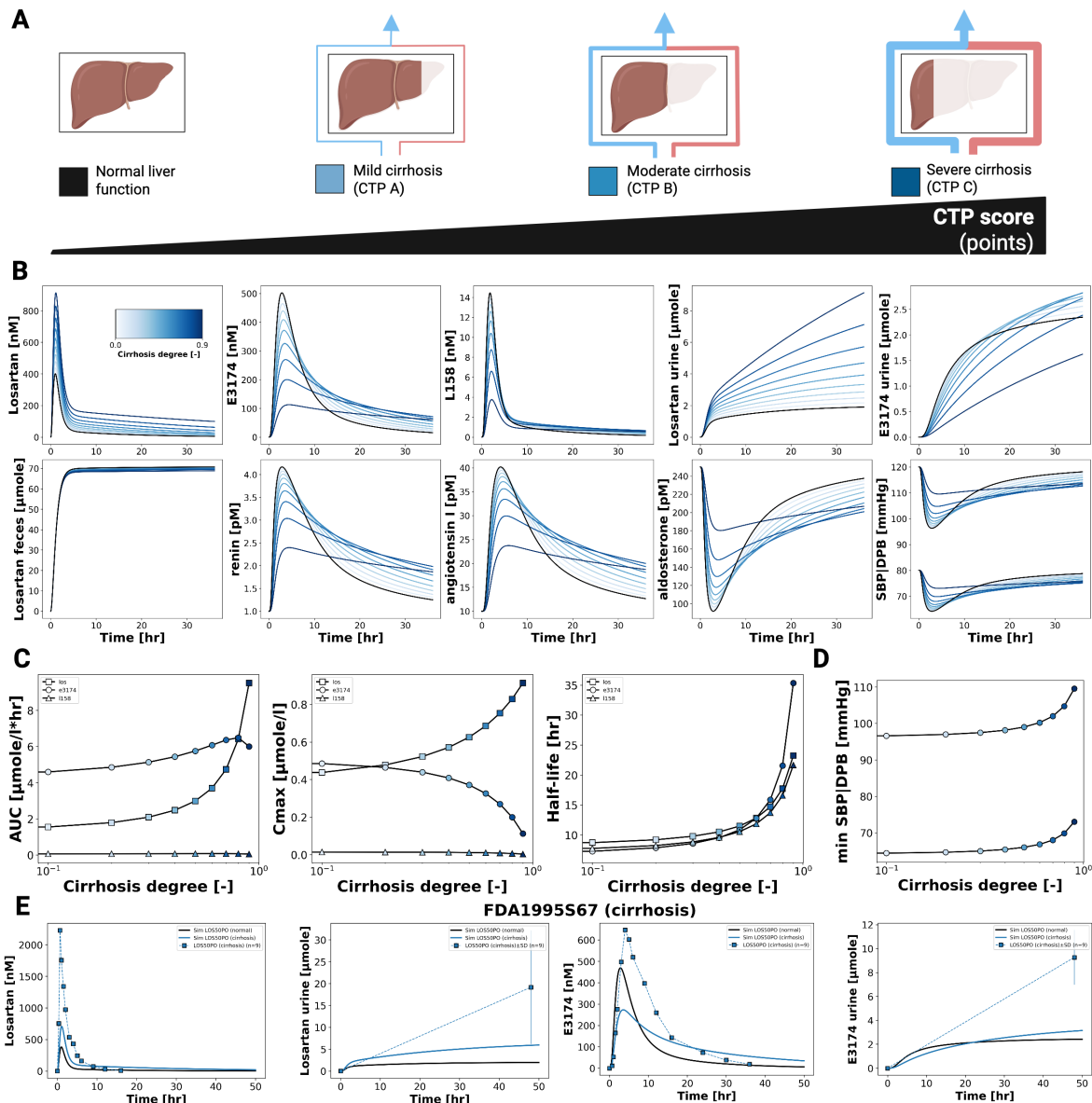


Figure 5. Effect of hepatic impairment on losartan pharmacokinetic and pharmacodynamic profiles. (A) Illustration of the level of cirrhosis evaluated in the simulations. (B) Simulated plasma concentrations profiles of losartan, E3174 and L158, urinary excretion profile of losartan and E3174, a fecal excretion profile of losartan, as well as simulated RAAS biomarkers (renin, angiotensin I and aldosterone) and blood pressure responses across cirrhosis degrees. Cirrhosis degree is indicated by line color. (C) Cirrhosis degree-dependent curves for AUC, C_{\max} and half-life. (D) Cirrhosis degree-dependent maximum or minimum values of systolic blood pressure SBP and diastolic blood pressure DBP. (E) Simulated (solid lines) versus observed (symbols) pharmacodynamic timecourses for different degrees of cirrhosis in FDA1995S67 [77].

Pharmacodynamically, lower CYP2C9 activity diminishes RAAS inhibition, with smaller reductions in aldosterone and systolic blood pressure, and attenuated compensatory increases in renin and angiotensin I. AUC and C_{\max} for losartan rise with declining enzyme activity, while E3174 exposure decreases; elimination rate constants and half-life remain relatively stable. These model predictions are consistent with clinical observations, which report 1.6- to 3-fold increases in losartan AUC and significantly reduced E3174 levels in carriers of reduced-function alleles [35–37], although absolute concentrations tend to be slightly underestimated.

The use of a continuous CYP2C9 activity scale enables the simulation of nonlinear relationships between enzyme activity and metabolite formation across a spectrum of genotypes. While CYP2C9 genotype is a major determinant of inter-individual variability, other factors such as age, comorbidities,

197

198

199

200

201

202

203

204

205

206

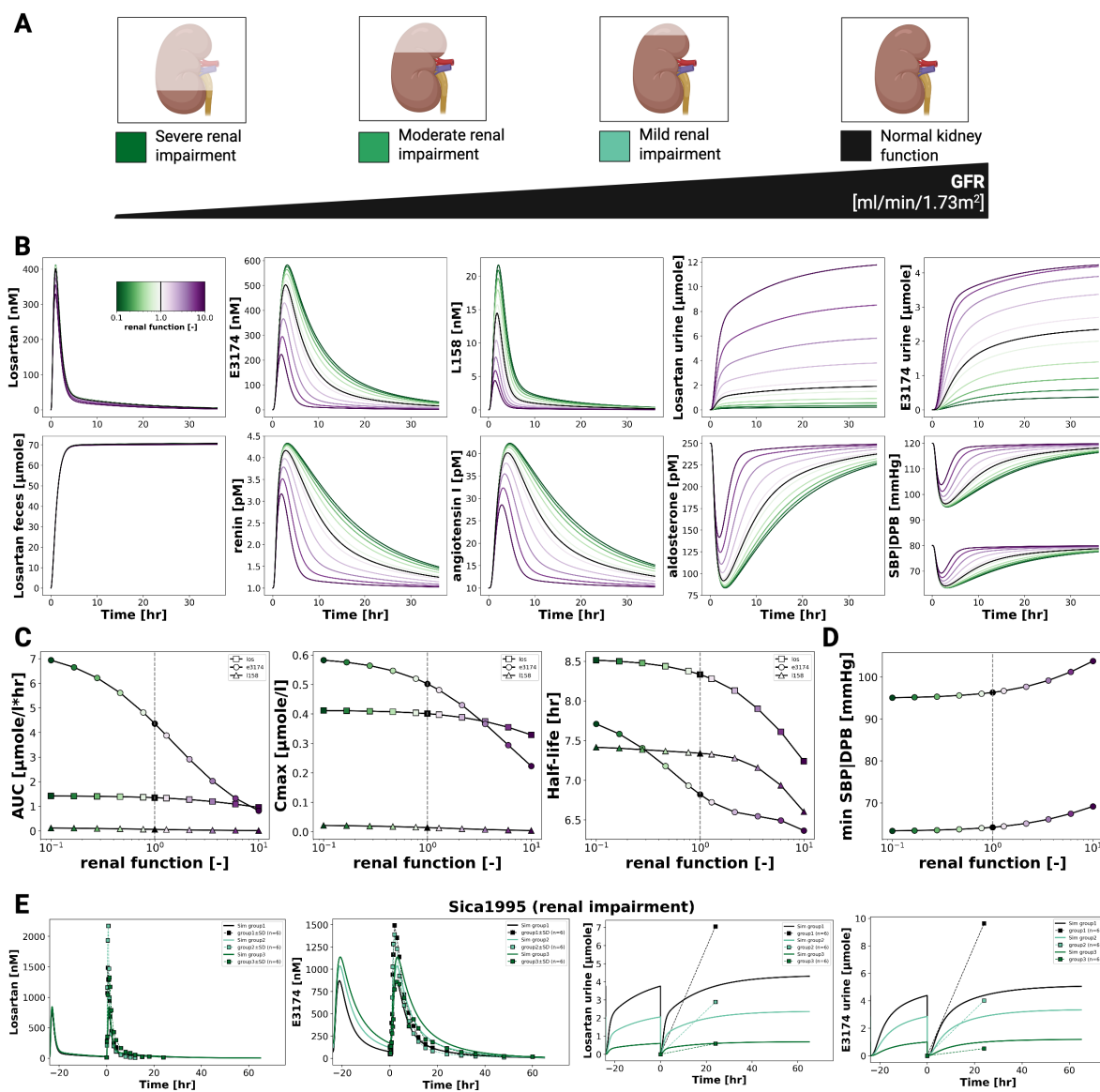


Figure 6. Effect of renal impairment on losartan pharmacokinetics and pharmacodynamic profiles. (A) Illustration of the level of renal impairment evaluated in the simulations. (B) Simulated plasma concentrations profiles of losartan, E3174 and L158, urinary excretion profile of losartan and E3174, a fecal excretion profile of losartan, as well as simulated RAAS biomarkers (renin, angiotensin I and aldosterone) and blood pressure responses across degrees of renal function. Renal function degree is indicated by line color. (C) Renal function-dependent curves for AUC, C_{max} and half-life. (D) Renal function-dependent maximum or minimum values of systolic blood pressure SBP and diastolic blood pressure DBP. (E) Simulated (solid lines) versus observed (symbols) pharmacokinetic timecourses for different degrees of renal impairment in Sica1995 [19].

and concomitant medications may further influence pharmacokinetics and pharmacodynamics. From a clinical perspective, these findings support the potential of genotype-guided dosing for patients with reduced-function alleles, although high variability within genotype groups suggests that genetic testing should be applied selectively, focusing on individuals with inadequate response or elevated risk of adverse effects.

207

208

209

210

211

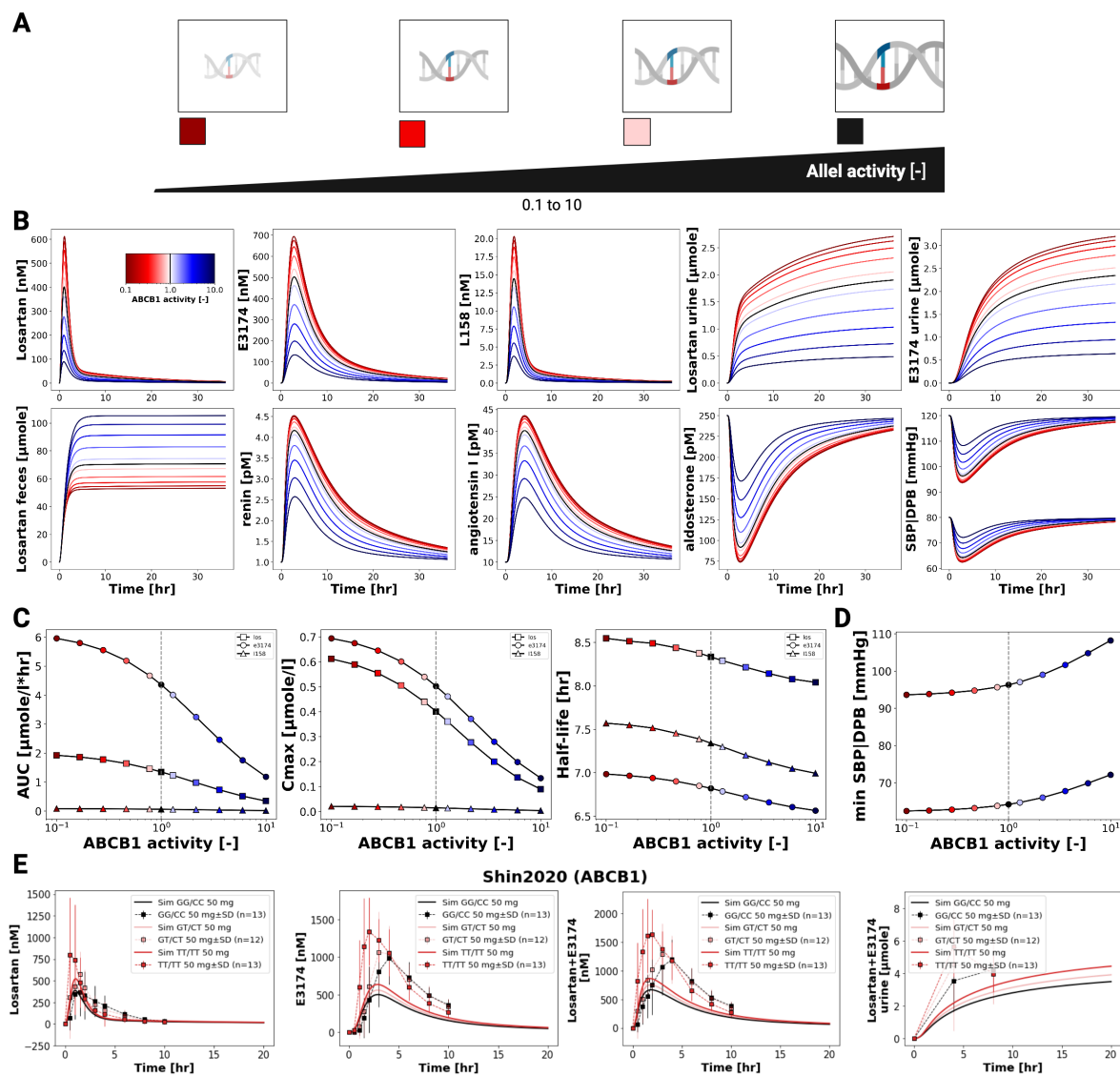


Figure 7. Pharmacokinetics and pharmacodynamics of losartan and metabolites across varying ABCB1 activity levels (A) Illustration of the level of CYP2C9 activity evaluated in the simulations. (B) Simulated plasma concentrations and excretion profiles of losartan, E3174 and L158, urinary excretion profile of losartan and E3174, a fecal excretion profile of losartan, as well as simulated RAAS biomarkers (renin, angiotensin I and aldosterone) and blood pressure responses across varying ABCB1 activity. Allel function degree is indicated by color. (C) ABCB1 activity-dependent curves for AUC, C_{\max} , elimination rate constant k_e , and half-life. (D) ABCB1 allele activity-dependent maximum or minimum values of systolic blood pressure SBP and diastolic blood pressure DBP. (E) Simulated (solid lines) versus observed (symbols) pharmacodynamic timecourses for different degrees of ABCB1 activity in Shin2020 [32].

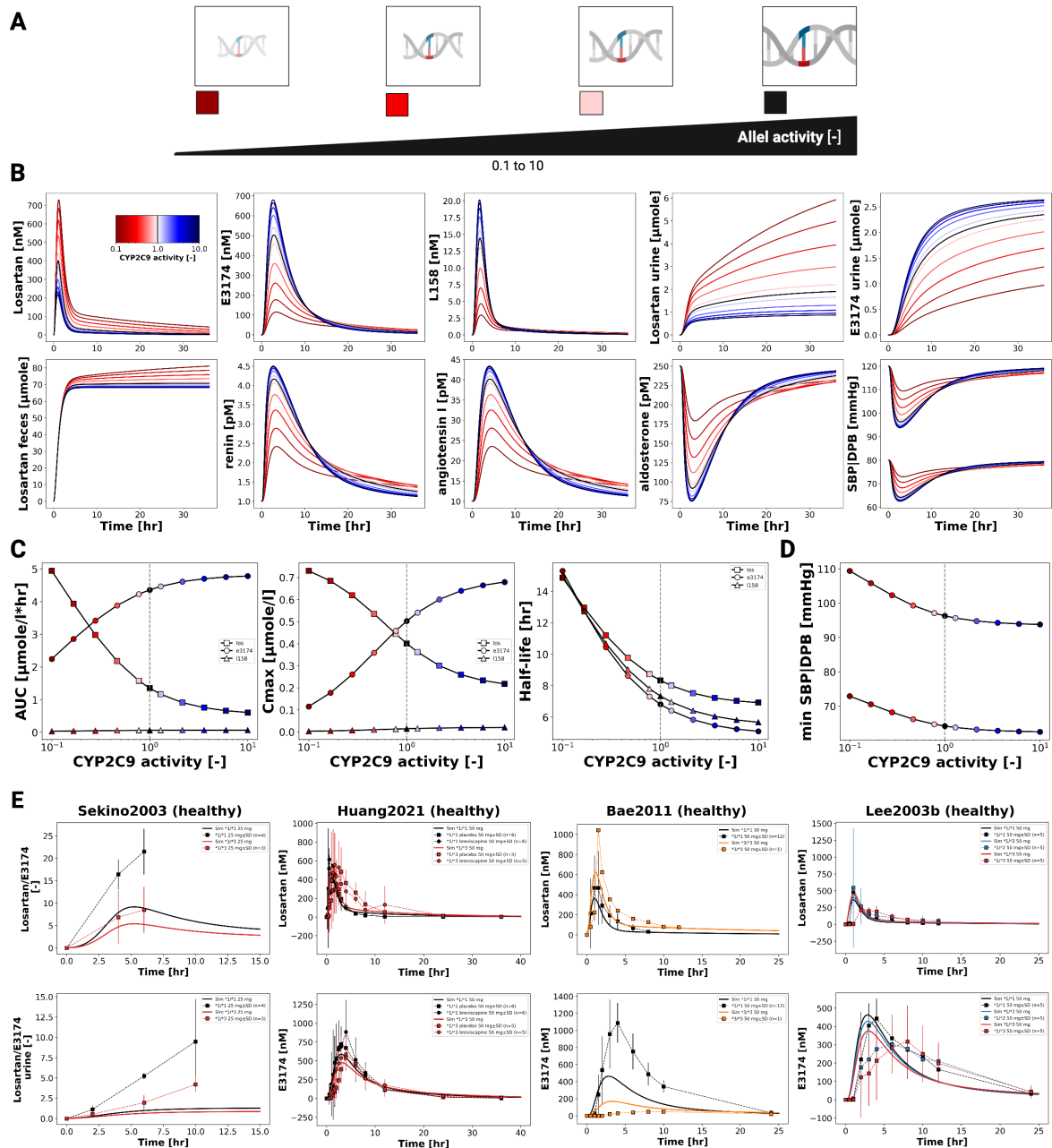


Figure 8. Pharmacokinetics and pharmacodynamics of losartan and metabolites across varying CYP2C9 activity levels. (A) Illustration of the level of CYP2C9 activity evaluated in the simulations. (B) Simulated plasma concentrations and excretion profiles of losartan, E3174, L158 and E3174/losartan ratio under varying CYP2C9 activity. (C) CYP2C9 activity-dependent curves for AUC, C_{\max} , elimination rate constant k_{el} , and half-life. (D) CYP2C9 allel activity-dependent maximum or minimum values of systolic blood pressure SBP and diastolic blood pressure DBP. (E) Simulated versus observed losartan pharmacokinetics. Data from [36,64,67,70].

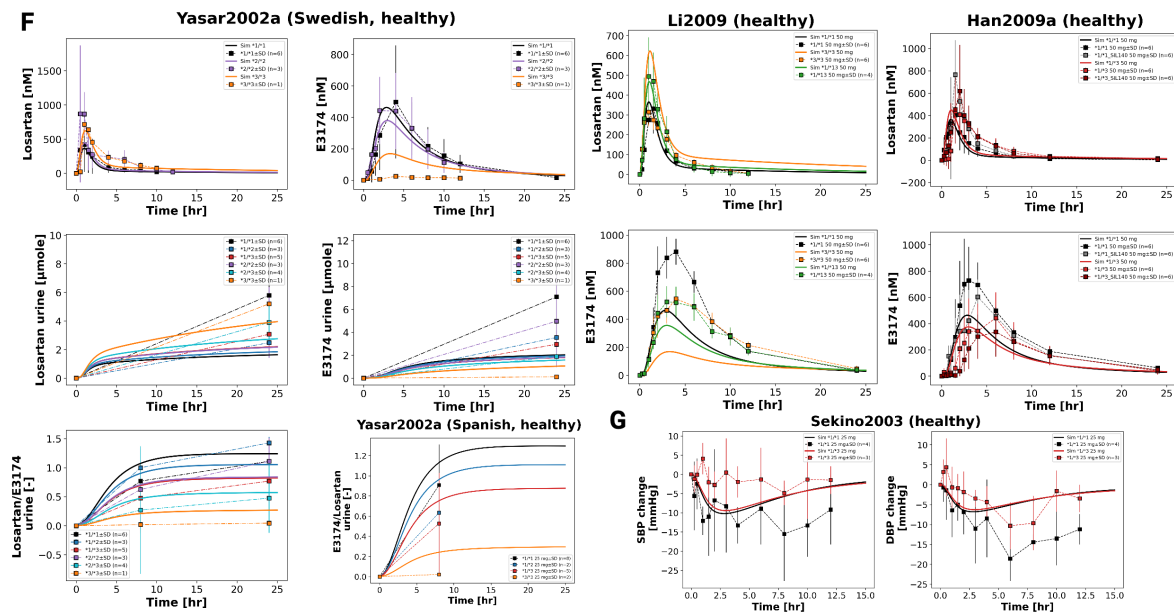


Figure 9. continued: Pharmacokinetics and pharmacodynamics of losartan and metabolites across varying CYP2C9 activity levels. **(F)** Simulated versus observed losartan pharmacokinetics. Data from [35,40,66]. Simulated versus observed SBP and DBP for different CYP2C9 genotypes [36].

4. Discussion

In this study, we developed and evaluated a physiologically based pharmacokinetic/ pharmacodynamic (PBPK/PD) model of losartan, informed by a curated database of 24 clinical studies covering diverse dosing regimens, populations, and physiological conditions. The model integrates intestinal absorption, hepatic metabolism via CYP2C9, and renal excretion, while linking systemic exposure of the active metabolite E3174 to downstream pharmacodynamic effects through a simplified RAAS submodel. This framework enables simulation of losartan and metabolite concentrations in plasma, urine, and feces, as well as prediction of pharmacodynamic endpoints such as renin, angiotensin I, aldosterone, and systolic blood pressure under baseline and perturbed conditions. By reproducing key clinical observations, the model demonstrates its potential to provide mechanistic insights into inter-individual variability and support personalized dosing strategies.

The curated database was essential for calibration and validation of the model, but it also highlights important limitations. While losartan pharmacokinetics are well characterized, data on RAAS dynamics remain limited, particularly with respect to circadian variability and long-term feedback regulation. Excretion data—especially for fecal elimination and the secondary metabolite L158—were sparse, and pharmacodynamic datasets showed high variability across studies. These gaps restrict the predictive accuracy of the model under complex physiological conditions but do not preclude its use in capturing system-level dose–exposure–response relationships.

Our dose dependency simulations reproduced the nonlinear pharmacokinetics of losartan and E3174, demonstrating a decreasing metabolite-to-parent ratio at higher doses due to saturable CYP2C9 metabolism. Consistent with clinical findings, increasing doses resulted in stronger and more sustained suppression of aldosterone and systolic blood pressure, accompanied by compensatory increases in renin and angiotensin I. This supports the model’s ability to capture both nonlinear PK behavior and dose-dependent RAAS responses.

In hepatic impairment, the model predicted elevated losartan plasma concentrations, reduced clearance, and attenuated metabolite formation, reflecting impaired CYP2C9 metabolism and hepatic blood flow. While the model underestimated the reported accumulation of E3174 in cirrhosis, it nonetheless confirmed the need for dose reduction in patients with liver dysfunction, particularly in comorbid conditions such as heart failure where sensitivity to RAAS inhibition is heightened.

Renal impairment simulations predicted reduced clearance of both losartan and E3174, leading to prolonged systemic exposure. While these results are qualitatively consistent with PK data, the model overestimated E3174 accumulation compared to reported clinical findings. Importantly, in the absence of PD data from impaired populations, the model allowed prediction of enhanced RAAS suppression and blood pressure reduction—although these effects may be slightly exaggerated due to the omission of compensatory mechanisms.

Genetic variability was also explored. For CYP2C9, the model captured the pronounced impact of reduced-function alleles on E3174 formation and downstream pharmacodynamic effects, reproducing the diminished blood pressure reduction observed clinically. The use of a continuous enzyme activity scale enabled simulation across a spectrum of genotypic variability. In contrast, ABCB1 (P-gp) variability had only minor effects on systemic exposure and blood pressure, consistent with limited clinical data, although the model suggests possible contributions via altered intestinal efflux and renal secretion. These findings emphasize the potential of PBPK/PD modeling to disentangle the contributions of genetic variability to losartan response.

Looking forward, several opportunities for refinement exist. Incorporating circadian rhythm, sodium and water balance, and autonomic feedback would enhance physiological fidelity of the RAAS submodel. Expanding datasets for fecal excretion, L158 kinetics, and pharmacodynamic outcomes would strengthen calibration. Future model extensions could also integrate additional sources of variability, such as age, comorbidities, or transporter–enzyme interactions, to support population-level simulations. Ultimately, the losartan PBPK/PD framework provides a mechanistically grounded

platform for exploring inter-individual variability and optimizing dosing strategies, with potential applications in precision medicine and clinical decision support. 261
262

5. Conclusions 263

In this study, a comprehensive physiologically based pharmacokinetic/ pharmacodynamic (PBPK/PD) model of losartan was developed and validated using an extensive clinical database. The model successfully reproduced key pharmacokinetic and pharmacodynamic behaviors, including dose-dependent RAAS inhibition and nonlinear metabolite formation resulting from saturable CYP2C9 metabolism. Simulations captured the attenuated pharmacodynamic response under hepatic impairment and predicted enhanced RAAS suppression in renal dysfunction. Furthermore, the model quantified the pronounced impact of CYP2C9 genetic variability on metabolite exposure and blood pressure effects, while ABCB1 activity contributed only minor modulation of systemic exposure. 264
265
266
267
268
269
270
271

Despite certain limitations in clinical data and model scope, the framework provides valuable mechanistic insight into inter-individual variability in losartan response. It highlights the potential of systems pharmacology modeling to support dose optimization across physiological and genetic conditions. Together, the losartan database and PBPK/PD model establish a solid foundation for future integration into digital twin platforms and personalized therapy design. 272
273
274
275
276

Author Contributions: Conceptualization, M.K.; methodology, M.K.; software, M.K.; validation, M.K.; formal analysis, E.T.; investigation, E.T.; resources, M.K.; data curation, E.T., M.K.; writing—original draft preparation, E.T.; writing—review and editing, M.K., E.T.; visualization, M.K.; supervision, M.K.; project administration, M.K.; funding acquisition, M.K. All authors have read and agreed to the published version of the manuscript. 277
278
279
280

Funding: M.K. was supported by the BMBF grant number 031L0304B and by the DFG grant number 436883643 281
and 465194077. 282

Data Availability Statement: All curated pharmacokinetic data are publicly available in the PK-DB database 283 (<https://pk-db.com>). The model and all associated materials (simulation scripts, parameters, and documentation) 284 are publicly available in SBML format under a CC-BY 4.0 license at <https://github.com/matthiaskoenig/losartan-model> [52]. 285
286

Acknowledgments: This work was supported by the BMBF-funded de.NBI Cloud within the German Network 287 for Bioinformatics Infrastructure (de.NBI) (031A537B, 031A533A, 031A538A, 031A533B, 031A535A, 031A537C, 288 031A534A, 031A532B). 289

Conflicts of Interest: The authors declare no conflicts of interest. 290

References 291

- (WHO), W.H.O. Hypertension. <https://www.who.int/news-room/fact-sheets/detail/hypertension>, 2023. 292
- NCD Risk Factor Collaboration (NCD-RisC). Worldwide Trends in Hypertension Prevalence and Progress in Treatment and Control from 1990 to 2019: A Pooled Analysis of 1201 Population-Representative Studies with 104 Million Participants. *Lancet (London, England)* **2021**, *398*, 957–980. [https://doi.org/10.1016/S0140-6736\(21\)01330-1](https://doi.org/10.1016/S0140-6736(21)01330-1). 293
294
295
296
- Fuchs, F.D.; Whelton, P.K. High Blood Pressure and Cardiovascular Disease. *Hypertension (Dallas, Tex.: 1979)* **2020**, *75*, 285–292. <https://doi.org/10.1161/HYPERTENSIONAHA.119.14240>. 297
298
- Fountain, J.H.; Kaur, J.; Lappin, S.L. Physiology, Renin Angiotensin System. In *StatPearls*; StatPearls Publishing: Treasure Island (FL), 2024. 299
300
- Atlas, S.A. The Renin-Angiotensin Aldosterone System: Pathophysiological Role and Pharmacologic Inhibition. *Journal of Managed Care Pharmacy* **2007**, *13*, 9–20. <https://doi.org/10.18553/jmcp.2007.13.s8-b.9>. 301
302
- Kotecha, D.; Flather, M.D.; Altman, D.G.; Holmes, J.; Rosano, G.; Wikstrand, J.; Packer, M.; Coats, A.J.S.; Manzano, L.; Böhm, M.; et al. Heart Rate and Rhythm and the Benefit of Beta-Blockers in Patients With Heart Failure. *Journal of the American College of Cardiology* **2017**, *69*, 2885–2896. <https://doi.org/10.1016/j.jacc.2017.04.001>. 303
304
305
306
- Ferrari, R. RAAS Inhibition and Mortality in Hypertension. *Global Cardiology Science and Practice* **2013**, *2013*, 34. <https://doi.org/10.5339/gcsp.2013.34>. 307
308

8. Burnier, M.; Wuerzner, G. Pharmacokinetic Evaluation of Losartan. *Expert opinion on drug metabolism & toxicology* **2011**, *7*, 643–649. <https://doi.org/10.1517/17425255.2011.570333>. 309
310
9. Bell, R.; Mandalia, R. Diuretics and the Kidney. *BJA education* **2022**, *22*, 216–223. <https://doi.org/10.1016/j.bjae.2022.02.003>. 311
312
10. Jones, K.E.; Hayden, S.L.; Meyer, H.R.; Sandoz, J.L.; Arata, W.H.; Dufrene, K.; Ballaera, C.; Lopez Torres, Y.; Griffin, P.; Kaye, A.M.; et al. The Evolving Role of Calcium Channel Blockers in Hypertension Management: Pharmacological and Clinical Considerations. *Current Issues in Molecular Biology* **2024**, *46*, 6315–6327. <https://doi.org/10.3390/cimb46070377>. 313
314
315
316
11. Sica, D.A.; Gehr, T.W.B.; Ghosh, S. Clinical Pharmacokinetics of Losartan. *Clinical pharmacokinetics* **2005**, *44*, 797–814. <https://doi.org/10.2165/00003088-200544080-00003>. 317
318
12. FDA. Cozaar Labeling-Package Insert. https://www.accessdata.fda.gov/drugsatfda_docs/label/2021/020386s064lbl.pdf, 2021. 319
320
13. Lo, M.W.; Goldberg, M.R.; McCrea, J.B.; Lu, H.; Furtek, C.I.; Bjornsson, T.D. Pharmacokinetics of Losartan, an Angiotensin II Receptor Antagonist, and Its Active Metabolite EXP3174 in Humans. *Clinical pharmacology and therapeutics* **1995**, *58*, 641–649. [https://doi.org/10.1016/0009-9236\(95\)90020-9](https://doi.org/10.1016/0009-9236(95)90020-9). 321
322
323
14. Goa, K.L.; Wagstaff, A.J. Losartan Potassium: A Review of Its Pharmacology, Clinical Efficacy and Tolerability in the Management of Hypertension. *Drugs* **1996**, *51*, 820–845. <https://doi.org/10.2165/00003495-199651050-00008>. 324
325
326
15. Flynn, C.A.; Hagenbuch, B.A.; Reed, G.A. Losartan Is a Substrate of Organic Anion Transporting Polypeptide 2B1. *The FASEB Journal* **2010**, *24*. https://doi.org/10.1096/fasebj.24.1_supplement.758.2. 327
328
16. Ohtawa, M.; Takayama, F.; Saitoh, K.; Yoshinaga, T.; Nakashima, M. Pharmacokinetics and Biochemical Efficacy after Single and Multiple Oral Administration of Losartan, an Orally Active Nonpeptide Angiotensin II Receptor Antagonist, in Humans. *British journal of clinical pharmacology* **1993**, *35*, 290–297. <https://doi.org/10.1111/j.1365-2125.1993.tb05696.x>. 329
330
331
332
17. Christ, D.D. Human Plasma Protein Binding of the Angiotensin II Receptor Antagonist Losartan Potassium (DuP 753/MK 954) and Its Pharmacologically Active Metabolite EXP3174. *Journal of clinical pharmacology* **1995**, *35*, 515–520. <https://doi.org/10.1002/j.1552-4604.1995.tb04097.x>. 333
334
335
18. FDA. 020386Orig1s000rev - COZAAR FDA Review. https://www.accessdata.fda.gov/drugsatfda_docs/nda/96/020386Orig1s000rev.pdf, 1995. 336
337
19. Sica, D.A.; Lo, M.W.; Shaw, W.C.; Keane, W.F.; Gehr, T.W.; Halstenson, C.E.; Lipschutz, K.; Furtek, C.I.; Ritter, M.A.; Shahinfar, S. The Pharmacokinetics of Losartan in Renal Insufficiency. *Journal of hypertension. Supplement : official journal of the International Society of Hypertension* **1995**, *13*, S49–52. <https://doi.org/10.1097/00004872-199507001-00007>. 338
339
340
341
20. Alonen, A.; Finel, M.; Kostiainen, R. The Human UDP-glucuronosyltransferase UGT1A3 Is Highly Selective towards N2 in the Tetrazole Ring of Losartan, Candesartan, and Zolarsartan. *Biochemical pharmacology* **2008**, *76*, 763–772. <https://doi.org/10.1016/j.bcp.2008.07.006>. 342
343
344
21. Williams, G.H. Aldosterone Biosynthesis, Regulation, and Classical Mechanism of Action. *Heart Failure Reviews* **2005**, *10*, 7–13. <https://doi.org/10.1007/s10741-005-2343-3>. 345
346
22. Rossi, G.P.; Lenzini, L.; Caroccia, B.; Rossitto, G.; Seccia, T.M. Angiotensin Peptides in the Regulation of Adrenal Cortical Function. *Exploration of Medicine* **2021**, *2*, 294–304. <https://doi.org/10.37349/emed.2021.0047>. 347
348
349
23. Rajamohan, S.B.; Raghuraman, G.; Prabhakar, N.R.; Kumar, G.K. NADPH Oxidase-Derived H(2)O(2) Contributes to Angiotensin II-induced Aldosterone Synthesis in Human and Rat Adrenal Cortical Cells. *Antioxidants & Redox Signaling* **2012**, *17*, 445–459. <https://doi.org/10.1089/ars.2011.4176>. 350
351
352
24. Neubauer, B.; Schrankl, J.; Steppan, D.; Neubauer, K.; Sequeira-Lopez, M.L.; Pan, L.; Gomez, R.A.; Coffman, T.M.; Gross, K.W.; Kurtz, A.; et al. Angiotensin II Short-Loop Feedback: Is There a Role of Ang II for the Regulation of the Renin System In Vivo? *Hypertension (Dallas, Tex.: 1979)* **2018**, *71*, 1075–1082. <https://doi.org/10.1161/HYPERTENSIONAHA.117.10357>. 353
354
355
356
25. Kammerl, M.C.; Richthammer, W.; Kurtz, A.; Krämer, B.K. Angiotensin II Feedback Is a Regulator of Renocortical Renin, COX-2, and nNOS Expression. *American Journal of Physiology-Regulatory, Integrative and Comparative Physiology* **2002**, *282*, R1613–R1617. <https://doi.org/10.1152/ajpregu.00464.2001>. 357
358
359
26. Gigante, B.; Piras, O.; De Paolis, P.; Porcellini, A.; Natale, A.; Volpe, M. Role of the Angiotensin II AT2-subtype Receptors in the Blood Pressure-Lowering Effect of Losartan in Salt-Restricted Rats. *Journal of Hypertension* **1998**, *16*, 2039–2043. <https://doi.org/10.1097/00004872-199816121-00027>. 360
361
362

27. McIntyre, M.; Caffe, S.E.; Michalak, R.A.; Reid, J.L. Losartan, an Orally Active Angiotensin (AT1) Receptor Antagonist: A Review of Its Efficacy and Safety in Essential Hypertension. *Pharmacology & therapeutics* **1997**, *74*, 181–194. [https://doi.org/10.1016/s0163-7258\(97\)82002-5](https://doi.org/10.1016/s0163-7258(97)82002-5). 363
364
365
28. Pedro, A.A.; Gehr, T.W.; Brophy, D.F.; Sica, D.A. The Pharmacokinetics and Pharmacodynamics of Losartan in Continuous Ambulatory Peritoneal Dialysis. *Journal of clinical pharmacology* **2000**, *40*, 389–395. <https://doi.org/10.1177/00912700022009099>. 366
367
368
29. Yoshitani, T.; Yagi, H.; Inotsume, N.; Yasuhara, M. Effect of Experimental Renal Failure on the Pharmacokinetics of Losartan in Rats. *Biological & pharmaceutical bulletin* **2002**, *25*, 1077–1083. <https://doi.org/10.1248/bpb.25.1077>. 369
370
371
30. Sica, D.A.; Halstenson, C.E.; Gehr, T.W.; Keane, W.F. Pharmacokinetics and Blood Pressure Response of Losartan in End-Stage Renal Disease. *Clinical pharmacokinetics* **2000**, *38*, 519–526. <https://doi.org/10.2165/00003088-200038060-00005>. 372
373
374
31. Göktas, M.T.; Pepedil, F.; Karaca, Ö.; Kalkışım, S.; Cevik, L.; Gumus, E.; Guven, G.S.; Babaoglu, M.O.; Bozkurt, A.; Yasar, U. Relationship between Genetic Polymorphisms of Drug Efflux Transporter MDR1 (ABCB1) and Response to Losartan in Hypertension Patients. *European Review for Medical and Pharmacological Sciences* **2016**, *20*, 2460–2467. 375
376
377
378
32. Shin, H.B.; Jung, E.H.; Kang, P.; Lim, C.W.; Oh, K.Y.; Cho, C.K.; Lee, Y.J.; Choi, C.I.; Jang, C.G.; Lee, S.Y.; et al. ABCB1 c.2677G>T/c.3435C>T Diplootype Increases the Early-Phase Oral Absorption of Losartan. *Archives of pharmacal research* **2020**, *43*, 1187–1196. <https://doi.org/10.1007/s12272-020-01294-3>. 379
380
381
33. Haufroid, V. Genetic Polymorphisms of ATP-binding Cassette Transporters ABCB1 and ABCC2 and Their Impact on Drug Disposition. *Current Drug Targets* **2011**, *12*, 631–646. <https://doi.org/10.2174/138945011795378487>. 382
383
384
34. Yasar, U.; Eliasson, E.; Forslund-Bergengren, C.; Tybring, G.; Gadd, M.; Sjöqvist, F.; Dahl, M.L. The Role of CYP2C9 Genotype in the Metabolism of Diclofenac in Vivo and in Vitro. *European journal of clinical pharmacology* **2001**, *57*, 729–735. <https://doi.org/10.1007/s00228-001-0376-7>. 385
386
387
35. Yasar, U.; Forslund-Bergengren, C.; Tybring, G.; Dorado, P.; Llerena, A.; Sjöqvist, F.; Eliasson, E.; Dahl, M.L. Pharmacokinetics of Losartan and Its Metabolite E-3174 in Relation to the CYP2C9 Genotype. *Clinical pharmacology and therapeutics* **2002**, *71*, 89–98. <https://doi.org/10.1067/mcp.2002.121216>. 388
389
390
36. Sekino, K.; Kubota, T.; Okada, Y.; Yamada, Y.; Yamamoto, K.; Horiuchi, R.; Kimura, K.; Iga, T. Effect of the Single CYP2C9*3 Allele on Pharmacokinetics and Pharmacodynamics of Losartan in Healthy Japanese Subjects. *European journal of clinical pharmacology* **2003**, *59*, 589–592. <https://doi.org/10.1007/s00228-003-0664-5>. 391
392
393
394
37. Fischer, T.L.; Pieper, J.A.; Graff, D.W.; Rodgers, J.E.; Fischer, J.D.; Parnell, K.J.; Goldstein, J.A.; Greenwood, R.; Patterson, J.H. Evaluation of Potential Losartan-Phenytoin Drug Interactions in Healthy Volunteers. *Clinical pharmacology and therapeutics* **2002**, *72*, 238–246. <https://doi.org/10.1067/mcp.2002.127945>. 395
396
397
38. Miners, J.O.; Birkett, D.J. Cytochrome P4502C9: An Enzyme of Major Importance in Human Drug Metabolism. *British Journal of Clinical Pharmacology* **1998**, *45*, 525–538. <https://doi.org/10.1046/j.1365-2125.1998.00721.x>. 398
399
400
39. Taube, J.; Halsall, D.; Baglin, T. Influence of Cytochrome P-450 CYP2C9 Polymorphisms on Warfarin Sensitivity and Risk of over-Anticoagulation in Patients on Long-Term Treatment. *Blood* **2000**, *96*, 1816–1819. 401
402
40. Li, Z.; Wang, G.; Wang, L.S.; Zhang, W.; Tan, Z.R.; Fan, L.; Chen, B.L.; Li, Q.; Liu, J.; Tu, J.H.; et al. Effects of the CYP2C9*13 Allele on the Pharmacokinetics of Losartan in Healthy Male Subjects. *Xenobiotica; the fate of foreign compounds in biological systems* **2009**, *39*, 788–793. <https://doi.org/10.1080/00498250903134435>. 403
404
405
41. Zhou, S.F.; Liu, J.P.; Chowbay, B. Polymorphism of Human Cytochrome P450 Enzymes and Its Clinical Impact. *Drug Metabolism Reviews* **2009**, *41*, 89–295. <https://doi.org/10.1080/03602530902843483>. 406
407
42. Gonzalez Hernandez, F.; Carter, S.J.; Iso-Sipilä, J.; Goldsmith, P.; Almousa, A.A.; Gastine, S.; Lilaonitkul, W.; Kloprogge, F.; Standing, J.F. An Automated Approach to Identify Scientific Publications Reporting Pharmacokinetic Parameters. *Wellcome Open Research* **2021**, *6*, 88. <https://doi.org/10.12688/wellcomeopenres.16718.1>. 408
409
410
411
43. Grzegorzewski, J.; Brandhorst, J.; Green, K.; Eleftheriadou, D.; Duport, Y.; Barthorscht, F.; Köller, A.; Ke, D.Y.J.; De Angelis, S.; König, M. PK-DB: Pharmacokinetics Database for Individualized and Stratified Computational Modeling. *Nucleic Acids Research* **2021**, *49*, D1358–D1364. <https://doi.org/10.1093/nar/gkaa990>. 412
413
414
415
44. Rohatgi, A. WebPlotDigitizer - a Computer Vision Assisted Software That Helps Extract Numerical Data from Images of a Variety of Data Visualizations, 2024. 416
417

45. Hucka, M.; Bergmann, F.T.; Chaouiya, C.; Dräger, A.; Hoops, S.; Keating, S.M.; König, M.; Novère, N.L.; Myers, C.J.; Olivier, B.G.; et al. The Systems Biology Markup Language (SBML): Language Specification for Level 3 Version 2 Core Release 2. *Journal of Integrative Bioinformatics* **2019**, *16*. <https://doi.org/10.1515/jib-2019-0021>. 418
419
420
421
46. Keating, S.M.; Waltemath, D.; König, M.; Zhang, F.; Dräger, A.; Chaouiya, C.; Bergmann, F.T.; Finney, A.; Gillespie, C.S.; Helikar, T.; et al. SBML Level 3: An Extensible Format for the Exchange and Reuse of Biological Models. *Molecular Systems Biology* **2020**, *16*, e9110. <https://doi.org/10.15252/msb.20199110>. 422
423
424
47. König, M. Sbmlutils: Python Utilities for SBML. Zenodo, 2024. <https://doi.org/10.5281/ZENODO.13325770>. 425
48. König, M.; Dräger, A.; Holzhütter, H.G. CySBML: A Cytoscape Plugin for SBML. *Bioinformatics* **2012**, *28*, 2402–2403. <https://doi.org/10.1093/bioinformatics/bts432>. 426
427
49. König, M. Sbmlsim: SBML Simulation Made Easy. Zenodo, 2021. <https://doi.org/10.5281/ZENODO.5531088>. 428
429
50. Welsh, C.; Xu, J.; Smith, L.; König, M.; Choi, K.; Sauro, H.M. libRoadRunner 2.0: A High Performance SBML Simulation and Analysis Library. *Bioinformatics* **2023**, *39*, btac770. <https://doi.org/10.1093/bioinformatics/btac770>. 430
431
432
51. Somogyi, E.T.; Bouteiller, J.M.; Glazier, J.A.; König, M.; Medley, J.K.; Swat, M.H.; Sauro, H.M. libRoadRunner: A High Performance SBML Simulation and Analysis Library. *Bioinformatics* **2015**, *31*, 3315–3321. <https://doi.org/10.1093/bioinformatics/btv363>. 433
434
435
52. Tensil, E.; König, M. Physiologically Based Pharmacokinetic/ Pharmacodynamic (PBPK/PD) Model of Losartan. Zenodo, 2025. <https://doi.org/10.5281/zenodo.17288163>. 436
437
53. Köller, A.; Grzegorzewski, J.; König, M. Physiologically Based Modeling of the Effect of Physiological and Anthropometric Variability on Indocyanine Green Based Liver Function Tests. *Frontiers in Physiology* **2021**, *12*, 757293. <https://doi.org/10.3389/fphys.2021.757293>. 438
439
440
54. Köller, A.; Grzegorzewski, J.; Tautenhahn, H.M.; König, M. Prediction of Survival After Partial Hepatectomy Using a Physiologically Based Pharmacokinetic Model of Indocyanine Green Liver Function Tests. *Frontiers in Physiology* **2021**, *12*, 730418. <https://doi.org/10.3389/fphys.2021.730418>. 441
442
443
55. Child, C.G.; Turcotte, J.G. Surgery and Portal Hypertension. *Major Problems in Clinical Surgery* **1964**, *1*, 1–85. 444
56. Pugh, R.N.; Murray-Lyon, I.M.; Dawson, J.L.; Pietroni, M.C.; Williams, R. Transection of the Oesophagus for Bleeding Oesophageal Varices. *The British Journal of Surgery* **1973**, *60*, 646–649. <https://doi.org/10.1002/bjs.1800600817>. 445
446
447
57. Stevens, P.E.; Ahmed, S.B.; Carrero, J.J.; Foster, B.; Francis, A.; Hall, R.K.; Herrington, W.G.; Hill, G.; Inker, L.A.; Kazancıoğlu, R.; et al. KDIGO 2024 Clinical Practice Guideline for the Evaluation and Management of Chronic Kidney Disease. *Kidney International* **2024**, *105*, S117–S314. <https://doi.org/10.1016/j.kint.2023.10.018>. 448
449
450
451
58. Mallol, B.S.; Grzegorzewski, J.; Tautenhahn, H.M.; König, M. Insights into Intestinal P-glycoprotein Function Using Talinolol: A PBPK Modeling Approach, 2023. <https://doi.org/10.1101/2023.11.21.568168>. 452
453
59. Maekawa, K.; Harakawa, N.; Sugiyama, E.; Tohkin, M.; Kim, S.R.; Kaniwa, N.; Katori, N.; Hasegawa, R.; Yasuda, K.; Kamide, K.; et al. Substrate-Dependent Functional Alterations of Seven CYP2C9 Variants Found in Japanese Subjects. *Drug Metabolism and Disposition: The Biological Fate of Chemicals* **2009**, *37*, 1895–1903. <https://doi.org/10.1124/dmd.109.027003>. 454
455
456
457
60. Kusama, M.; Maeda, K.; Chiba, K.; Aoyama, A.; Sugiyama, Y. Prediction of the Effects of Genetic Polymorphism on the Pharmacokinetics of CYP2C9 Substrates from in Vitro Data. *Pharmaceutical research* **2009**, *26*, 822–835. <https://doi.org/10.1007/s11095-008-9781-2>. 458
459
460
61. Wang, Y.H.; Pan, P.P.; Dai, D.P.; Wang, S.H.; Geng, P.W.; Cai, J.P.; Hu, G.X. Effect of 36 CYP2C9 Variants Found in the Chinese Population on Losartan Metabolism in Vitro. *Xenobiotica; the fate of foreign compounds in biological systems* **2014**, *44*, 270–275. <https://doi.org/10.3109/00498254.2013.820007>. 461
462
463
62. Hoffmeyer, S.; Burk, O.; von Richter, O.; Arnold, H.P.; Brockmöller, J.; Johne, A.; Cascorbi, I.; Gerloff, T.; Roots, I.; Eichelbaum, M.; et al. Functional Polymorphisms of the Human Multidrug-Resistance Gene: Multiple Sequence Variations and Correlation of One Allele with P-glycoprotein Expression and Activity in Vivo. *Proceedings of the National Academy of Sciences of the United States of America* **2000**, *97*, 3473–3478. <https://doi.org/10.1073/pnas.97.7.3473>. 464
465
466
467
468
63. Siegmund, W.; Ludwig, K.; Giessmann, T.; Dazert, P.; Schroeder, E.; Sperker, B.; Warzok, R.; Kroemer, H.K.; Cascorbi, I. The Effects of the Human MDR1 Genotype on the Expression of Duodenal P-glycoprotein and Disposition of the Probe Drug Talinolol. *Clinical Pharmacology and Therapeutics* **2002**, *72*, 572–583. <https://doi.org/10.1067/mcp.2002.127739>. 469
470
471
472

64. Bae, J.w.; Choi, C.i.; Kim, M.j.; Oh, D.h.; Keum, S.k.; Park, J.i.; Kim, B.h.; Bang, H.k.; Oh, S.g.; Kang, B.s.; et al. Frequency of CYP2C9 Alleles in Koreans and Their Effects on Losartan Pharmacokinetics. *Acta pharmacologica Sinica* **2011**, *32*, 1303–1308. <https://doi.org/10.1038/aps.2011.100>. 473
474
475
65. Donzelli, M.; Derungs, A.; Serratore, M.G.; Noppen, C.; Nezic, L.; Krähenbühl, S.; Haschke, M. The Basel Cocktail for Simultaneous Phenotyping of Human Cytochrome P450 Isoforms in Plasma, Saliva and Dried Blood Spots. *Clinical pharmacokinetics* **2014**, *53*, 271–282. <https://doi.org/10.1007/s40262-013-0115-0>. 476
477
478
66. Han, Y.; Guo, D.; Chen, Y.; Chen, Y.; Tan, Z.R.; Zhou, H.H. Effect of Silymarin on the Pharmacokinetics of Losartan and Its Active Metabolite E-3174 in Healthy Chinese Volunteers. *European journal of clinical pharmacology* **2009**, *65*, 585–591. <https://doi.org/10.1007/s00228-009-0624-9>. 479
480
481
67. Huang, H.X.; Wu, H.; Zhao, Y.; Zhou, T.; Ai, X.; Dong, Y.; Zhang, Y.; Lai, Y. Effect of CYP2C9 Genetic Polymorphism and Brevicaprime on Losartan Pharmacokinetics in Healthy Subjects. *Xenobiotica; the fate of foreign compounds in biological systems* **2021**, *51*, 616–623. <https://doi.org/10.1080/00498254.2021.1880670>. 482
483
484
68. Kim, M.G.; Kim, Y.; Jeon, J.Y.; Kim, D.S. Effect of Fermented Red Ginseng on Cytochrome P450 and P-glycoprotein Activity in Healthy Subjects, as Evaluated Using the Cocktail Approach. *British journal of clinical pharmacology* **2016**, *82*, 1580–1590. <https://doi.org/10.1111/bcp.13080>. 485
486
487
69. Kobayashi, M.; Takagi, M.; Fukumoto, K.; Kato, R.; Tanaka, K.; Ueno, K. The Effect of Bucolome, a CYP2C9 Inhibitor, on the Pharmacokinetics of Losartan. *Drug metabolism and pharmacokinetics* **2008**, *23*, 115–119. <https://doi.org/10.2133/dmpk.23.115>. 488
489
490
70. Lee, C.R.; Pieper, J.A.; Hinderliter, A.L.; Blaisdell, J.A.; Goldstein, J.A. Losartan and E3174 Pharmacokinetics in Cytochrome P450 2C9*1/*1, *1/*2, and *1/*3 Individuals. *Pharmacotherapy* **2003**, *23*, 720–725. <https://doi.org/10.1592/phco.23.6.720.32187>. 491
492
493
71. Munafo, A.; Christen, Y.; Nussberger, J.; Shum, L.Y.; Borland, R.M.; Lee, R.J.; Waeber, B.; Biollaz, J.; Brunner, H.R. Drug Concentration Response Relationships in Normal Volunteers after Oral Administration of Losartan, an Angiotensin II Receptor Antagonist. *Clinical pharmacology and therapeutics* **1992**, *51*, 513–521. <https://doi.org/10.1038/clpt.1992.56>. 494
495
496
497
72. Oh, K.S.; Park, S.J.; Shinde, D.D.; Shin, J.G.; Kim, D.H. High-Sensitivity Liquid Chromatography-Tandem Mass Spectrometry for the Simultaneous Determination of Five Drugs and Their Cytochrome P450-specific Probe Metabolites in Human Plasma. *Journal of chromatography. B, Analytical technologies in the biomedical and life sciences* **2012**, *895–896*, 56–64. <https://doi.org/10.1016/j.jchromb.2012.03.014>. 498
499
500
501
73. Puris, E.; Pasanen, M.; Ranta, V.P.; Gynther, M.; Petsalo, A.; Käkelä, P.; Männistö, V.; Pihlajamäki, J. Laparoscopic Roux-en-Y Gastric Bypass Surgery Influenced Pharmacokinetics of Several Drugs given as a Cocktail with the Highest Impact Observed for CYP1A2, CYP2C8 and CYP2E1 Substrates. *Basic & clinical pharmacology & toxicology* **2019**, *125*, 123–132. <https://doi.org/10.1111/bcpt.13234>. 502
503
504
505
74. Tanaka, S.; Uchida, S.; Inui, N.; Takeuchi, K.; Watanabe, H.; Namiki, N. Simultaneous LC-MS/MS Analysis of the Plasma Concentrations of a Cocktail of 5 Cytochrome P450 Substrate Drugs and Their Metabolites. *Biological & pharmaceutical bulletin* **2014**, *37*, 18–25. <https://doi.org/10.1248/bpb.b13-00401>. 506
507
508
75. Goldberg, M.R.; Bradstreet, T.E.; McWilliams, E.J.; Tanaka, W.K.; Lipert, S.; Bjornsson, T.D.; Waldman, S.A.; Osborne, B.; Pividori, L.; Lewis, G. Biochemical Effects of Losartan, a Nonpeptide Angiotensin II Receptor Antagonist, on the Renin-Angiotensin-Aldosterone System in Hypertensive Patients. *Hypertension (Dallas, Tex.: 1979)* **1995**, *25*, 37–46. <https://doi.org/10.1161/01.hyp.25.1.37>. 509
510
511
512
76. Doig, J.K.; MacFadyen, R.J.; Sweet, C.S.; Lees, K.R.; Reid, J.L. Dose-Ranging Study of the Angiotensin Type I Receptor Antagonist Losartan (DuP753/MK954), in Salt-Deplete Normal Man. *Journal of Cardiovascular Pharmacology* **1993**, *21*, 732–738. <https://doi.org/10.1097/00005344-199305000-00007>. 513
514
515
77. FDA. FDA1995S67 - 020386Orig1s000rev - COZAAR FDA Review. https://www.accessdata.fda.gov/drugsatfda_docs/nda/96/020386Orig1s000rev.pdf, 1995. 516
517